Molecular Dynamics Calculation of the Effect of Solvent Polarizability on the Hydrophobic Interaction

Michael H. New† and B. J. Berne*

Contribution from the Department of Chemistry and the Center for Biomolecular Simulation, Columbia University, New York, New York 10027

Received December 23, 1994®

Abstract: The potential of mean force (PMF) between two methane molecules in water is calculated using molecular dynamics with Ewald boundary conditions for two water models, the WK model (a nonpolarizable model) and the PSRWK model (a polarizable model), for the purpose of understanding what role many-body polarization plays in the hydrophobic interaction. These models of neat water have the same static dielectric constants and similar structural and thermodynamic properties. The methane−water interaction is taken to be exactly the same in both fluids. Nevertheless, the simulated potential of mean force between two dissolved methane molecules is very different for these two models. In the polarizable model, solvent-separated pairing is dominant over contact-pairing, while in the nonpolarizable model the reverse is true.

1. Introduction

Water reorganizes around small apolar solute molecules to form polyhedral cages or clathrates. Because the molar entropy of solvation of methane and inert gas atoms is negative it is thought that an apolar solute molecule orders water molecules causing the hydrogen bonds in its proximity to be stiffer than these in the bulk. When two apolar solutes are dissolved, the number of water molecules needed to solvate the pair in one cavity is smaller than the number of waters needed to form two single-solute cavities. Thus, the entropy of the system should be greater when the two solutes are in contact, that is, when they share a solvation cage, than when they are in separate, possibly connected, clathrate cages (the so called "solvent-separated pair"). It has thus been argued that there is an "entropic driving force" for hydrophobic aggregation. These considerations give rise to the traditional view that the hydrophobic effect is entropically driven; that is, the large entropy of association leads to a solvent-induced attraction between the solutes, at least at room temperature.

It should be stressed that entropically-driven aggregation should occur in the absence of any attractive interaction between the solute molecules. Attractive interactions between the solutes and the waters complicate the picture, however. Because more waters are involved in creating two separate hydration shells than in the contact pair state, the solvent-separated state will have more attractive water−solute interactions than the contact pair state and the solvation energy of the system will thus be lower in the solvent-separated state. In real systems, the hydrophobic effect arises from the competition between these two tendencies—enthalpically-driven disaggregation and entropically-driven aggregation.

Pratt and Chandler[1] constructed a semiempirical theory of the hydrophobic interaction between two hard-spheres based on the experimentally determined pair correlation function, $g_{OO}(r)$, of neat water. This theory predicted a potential of mean force between the two solutes that had two minima: one minimum corresponded to the contact pair and the other to the solvent-separated pair. The solvent-separated pair was found to be relatively more probable than the contact pair. If one labels the contact pair as X−X and the solvent-separated pair by X−H_2O−X, then the Pratt−Chandler PMF predicts[2] that the equilibrium constant for the reaction

$$X-X + H_2O \rightleftharpoons X-H_2O-X \qquad (1.1)$$

is $K_{eq} = 4.0$.

Pangali *et al.*[3] were the first to apply the techniques of computer simulation to the problem of hydrophobicity and to test Pratt and Chandler's theory. They computed the average force exerted by water, interacting through an ST2 potential,[4] on a pair of apolar spherical solute molecules parallel to the intermolecular axis for a set of fixed intersolute distances. Although they could not integrate their average force to yield an accurate estimate of the PMF, their data provided the first evidence in support of the existence of a strong solvent-separated minimum in the PMF.

Pangali *et al.* subsequently used umbrella sampling techniques to compute the potential of mean force.[2,5] Again two minima in the potential of mean force were found with solvent-separated pairing dominant over contact pairing. This was in qualitative agreement with the results of Pratt and Chandler's theory, although the equilibrium constant turned out to be $K_{eq} = 3$, a value somewhat smaller than that of Pratt and Chandler. Pangali *et al.* also examined the structure of the solvent-separated state and found that it usually consisted of the two solutes in individual clathrate cages with an intervening water shared between the two solvation shells.

Although not able to compute the PMF, Geiger *et al.*[6] simulated two neon-like particles in water, also using the ST2 model of water. Two solutes initially placed in contact were observed to vibrate for a very short time before separating and allowing one water molecule to penetrate the region between

† In partial fulfillment of the Ph.D. in the Department of Chemistry, Columbia University.

® Abstract published in *Advance ACS Abstracts*, June 15, 1995.

(1) Pratt, L. R.; Chandler, David *J. Chem. Phys.* **1977**, *67*(8), 3683−3704.

(2) Pangali, C.; Rao, M.; Berne, B. J. *J. Chem. Phys.* **1979**, *71*(7), 2975−2981.

(3) Pangali, C.; Rao, M.; Berne, B. J. ACS Symposium Series 86, 1978.

(4) Stillinger, F. H.; Scott, H. L. *J. Chem. Phys.* **1974**, *60*, 1545.

(5) Pangali, C.; Rao, M.; Berne, B. J. *J. Chem. Phys.* **1979**, *71*(7), 2982−2990.

(6) Geiger, A.; Rahman, A.; Stillinger, F. H. *J. Chem. Phys.* **1979**, *70*(1), 263−276.

0002-7863/95/1517-7172$09.00/0

them. This solvent-separated state persisted for the remainder of the simulation.

The existence and stability of the solvent-separated state has been confirmed by subsequent simulations using different pair-additive potentials.[7-9] Recently, Smith and Haymet[10] were able to determine the entropic and enthalpic parts of the PMF, $W(r) = \Delta H(r) - T\Delta S(r)$, and found that there was a strong entropic intersolute attraction at short separations and that the enthalpic contribution was everywhere positive and strongly repulsive in the region of the contact pair.

In all of the above cases, a stable minimum in the PMF corresponding to the solvent-separated pair has been found, and in all cases the solvent-separated pair was found to be more probable than the contact pair.

All of the above simulations are based on nonpolarizable pair water−water potentials like the SPC, TIP4P, and ST2 potentials in which the Lennard-Jones (LJ) parameters used to model the O−O short range interaction are fit to the measured enthalpy of vaporization of neat water without subtracting from this interaction either the polarization energy or the quantum librational energy. Recently water−water potentials have been reparametrized taking (some or all of) these contributions into account giving rise to the SPC/E and the WK potentials. In this paper we first examine whether the above observations regarding the hydrophobic interaction are robust against this reparametrization. We find that in the WK potential, contact pairing becomes dominant over solvent-separated pairing. It would be of interest to see if this reversal also holds true for the SPC/E potential.

The studies mentioned so far are based on nonpolarizable water models. The water molecule is small, polar, and polarizable. Upon condensation from the gas phase where the dipole moment is 1.87 D, an additional dipole moment of between 0.8 and 1.0 D is induced on average in every water molecule. One would therefore expect the charge distribution on a water to be sensitive to its surroundings thus giving rise to different energetics and orderings than in nonpolarizable models and perhaps leading to quite different hydrophobic interactions. Others[11] have disputed this contention.

Van Belle and Wodak,[12] in a recent simulation, have directly addressed the effects of solvent polarizability on the hydrophobic effect. They computed the PMF between two methanes for a nonpolarizable water model, SPC,[13] and a polarizable water model, PSPC.[14] They also investigated the solvent structure around the two solutes and around a single methane solute. Van Belle and Wodak found that in PSPC water the solvent separated minimum in the PMF is almost completely supressed.

To better understand the effect of solvent polarizability on the PMF for two apolar solutes in water, we report here a study in which we paid close attention to important details such as intermolecular potentials and the treatment of long-range forces. We compare the nonpolarizable water model of WK[15] with Sprik's polarizable PSRWK model.[16] Both models give excellent predictions for the thermodynamic and structural properties of bulk water and both also yield the correct static dielectric constant. Furthermore, both models possess the correct gas phase static quadrupole moment and adequately reproduce the structure of the water dimer. The Sprik model has a fixed dipole moment of 1.87 D augmented by a static dipole polarizability of 1.444 Å^3 and yields an average dipole in the bulk of 2.65 D. The WK model has a fixed dipole moment of 2.60 D, but its non-Coulombic parameters have been fit to a value of the internal energy which includes an approximation to the energy needed to polarize the water from its gas phase dipole moment.

In our studies we use the same potential parameters for the solute−water interactions for all models of water considered. These are the same as the parameters used by Smith and Haymet.[10] Finally, we have employed Ewald boundary conditions to account for the long-range nature of the Coulomb interaction. We also compare simulations based on spherically truncated potentials. These precautions should ensure that any differences in the computed potentials of mean force are due solely to the water potentials employed and are not artifacts of the simulation method.

It is shown in this study that our polarizable model (PSRWK) gives rise to much stronger solvent-separated pairing than our nonpolarizable model (WK). In our nonpolarizable model (WK) contact pairing is dominant over solvent-separated pairing, whereas in the polarizable model the reverse is observed. We suggest possible reasons for this behavior and compare and contrast it with previous work.[12]

2. Potential Models

2.1. The Sprik Polarizable Model of Water. The polarizable Sprik model (PSRWK) assigns four interaction sites to the water molecule. Positive partial charges, q_H, are placed at the positions of the hydrogens, and a compensating negative charge is placed on a site along the H−O−H bisector at a distance r_{OM} from the oxygen atom toward the hydrogen—the so-called "M" site. A fourth site is placed on each oxygen atom as the site for a Lennard-Jones interaction. The total interaction potential arising from the short range LJ potential and the interaction between the fixed or static charges is thus

$$U_{\text{static}} = \frac{1}{2}\sum_{i=1}^{N}\sum_{j=1}^{N}\left[\frac{A_{OO}}{||\mathbf{r}_{i,O} - \mathbf{r}_{j,O}||^{12}} - \frac{C_{OO}}{||\mathbf{r}_{i,O} - \mathbf{r}_{j,O}||^{6}}\right] + \frac{1}{2}\sum_{i=1}^{N}\sum_{j=1}^{N}\sum_{\alpha=H_1,H_2,M}\sum_{\beta=H_1,H_2,M}\frac{q_{i\alpha}q_{j\beta}}{||\mathbf{r}_{i,\alpha} - \mathbf{r}_{j,\beta}||} \quad (2.2)$$

The molecular polarizability of water is modeled by four closely spaced charges arranged in a tetrahedron centered on the oxygen, instead of by a point polarizability. Two of the charges point toward the hydrogen sites, while the other two point in the "lone pair" directions. The positions of these charges are fixed, but their magnitudes are free to fluctuate, subject to the constraint of zero total charge. The polarization energy of these fluctuating charges is taken to be[17]

$$U_{\text{pol}} = \sum_{i=1}^{N}\sum_{\alpha=1}^{4}\sum_{\beta=1}^{4}\frac{a^2}{2\alpha_0}q_{i\beta}C_{\beta\alpha}q_{i\alpha} \quad (2.3)$$

where α_0 is the isotropic dipole polarizability of a water molecule, the distance between the fluctuating charges is

(7) Rapaport, D. C.; Scheraga, H. A. *J. Phys. Chem.* **1982**, *86*(6), 873−880.
(8) Ravishankar, G.; Mezei, M.; Beveridge, D. L. *Faraday Symp. Chem. Soc.* **1982**, *17*, 79−91.
(9) Watanabe, K.; Andersen, H. C. *J. Phys. Chem.* **1986**, *90*(5), 795−802.
(10) Smith, David E.; Haymet, A. D. J. *J. Chem. Phys.* **1993**, *98*, 6445.
(11) Wallqvist, Anders *J. Phys. Chem.* **1991**, *95*(22), 8921−8927.
(12) van Belle, Daniel; Wodak, Shoshana J. *J. Am. Chem. Soc.* **1993**, *115*(2), 647−652.
(13) Berendsen, H. J. C.; Postma, J. P. M.; van Gunsteren, W. F.; Hermans, J. Reidel, 1981; p 331−342.
(14) Ahlström, Peter; Wallqvist, Anders; Engström, Sven; Jönsson, Bo *Mol. Phys.* **1989**, *68*(3), 563−581.
(15) Watanabe, Kyoko; Klein, Michael L. *Chem. Phys.* **1989**, *131*(2), 157−167.
(16) Sprik, Michiel *J. Chem. Phys.* **1991**, *95*(9), 6762−6769.
(17) Sprik, Michiel *J. Phys. Chem.* **1991**, *95*, 2283−2291.

Table 1. Comparison of the Parameters of the Sprik Model (PSRWK) and the Watanabe and Klein Model (WK)

parameter	WK	PSRWK
r_{OM} (Å)	0.15	0.26
q_H (e)	0.62	0.60
A_{OO} (10^6 kJ Å^{12} mol^{-1})	5.000	3.766
C_{OO} (10^3 kJ Å^6 mol^{-1})	4.850	3.556
a (Å)		0.20
α_0 (Å^3)		1.444
ξ (Å)		0.775

$\sqrt{2a}$, and $C_{\beta\alpha}$ are coupling constants. In order to provide for the short-range damping of polarization interactions, the fluctuating charges are "smeared" into Gaussian distributions of root mean square width ξ. This complicates the computation of interaction energies and forces. The Coulomb interaction between Gaussian charge distributions of widths ξ_i and ξ_j is given by

$$U = \frac{q_i q_j}{||\mathbf{r}_i - \mathbf{r}_j||} \operatorname{erf}\left(\frac{||\mathbf{r}_i - \mathbf{r}_j||}{\sqrt{2(\xi_i^2 + \xi_j^2)}}\right) \tag{2.4}$$

The total interaction potential consists of the sum of U_{static}, the Coulomb interactions between the Gaussian fluctuating charges and between the fluctuating charges and the fixed charges, and U_{pol}. The specific parameters of the polarizable (PSRWK) can be found in ref 16 and Table 1.

One method of obtaining the polarizable charges is to treat the extra charge degrees of freedom as dynamical variables by introducing a fictitious kinetic energy into the Lagrangian

$$T_{\text{fictitious}} = \sum_{i=1}^{N} \sum_{\alpha=1}^{4} m' \dot{q}_{i\alpha}^2/2 \tag{2.5}$$

where m' is a fictitious mass. Thus, standard molecular dynamics techniques, such as the velocity Verlet algorithm,[18] are used to propagate the induced charges forward in time in concert with the time evolution of the molecular positions and velocities.

The dynamics of the fluctuating charges is complicated by the intramolecular coupling, given by the $C_{\beta\alpha}$, and by the constraint of zero total charge. Both of these complications may be eliminated by a normal model transformation. The new variables, denoted by q_A, q_x, q_y, and q_z, are related to the old variables, q_1, q_2, q_3, and q_4 by[19]

$$\begin{aligned} q_A &= \tfrac{1}{2}(q_1 + q_2 + q_3 + q_4) \\ q_x &= \tfrac{1}{2}(q_1 - q_2 + q_3 - q_4) \\ q_y &= \tfrac{1}{2}(-q_1 - q_2 + q_3 + q_4) \\ q_z &= \tfrac{1}{2}(-q_1 + q_2 + q_3 - q_4) \end{aligned} \tag{2.6}$$

The charge distribution produced by the fluctuating charges gives rise to small multipolar polarizabilities in addition to the dipole polarizability. In terms of the transformed (normal mode) charges, the polarization potential becomes simply

$$U_{\text{pol}} = \sum_{i=1}^{N} \frac{a^2}{2\alpha_0}(q_{ix}^2 + q_{iy}^2 + q_{iz}^2) \tag{2.7}$$

The equations of motion for the transformed charges are then

$$m_Q \ddot{q}_{i\kappa} = -\frac{a^2}{\alpha_0} q_{i\kappa} + V_{i\kappa} \tag{2.8}$$

$$m_Q \ddot{q}_{iA} = -\frac{a^2}{\alpha_{0\kappa=1}} \sum^{4} q_{i\kappa} \tag{2.9}$$

where $\kappa = x, y, z$ and the $\{V_{i\kappa}\}$ are the result of applying the transformation of eq 2.7 to the intermolecular forces defined by

$$F_{i\alpha} = -\frac{\partial U_{es}}{\partial q_{i\alpha}}, \quad \alpha = 1, 2, 3, 4 \tag{2.10}$$

The constraint of zero total charge can now be trivially satisfied by starting the system in a state where each water molecule is neutral and then not integrating the equations of motion for the $\{q_{iA}\}$.

The partial charges and LJ parameters were chosen by Sprik to reproduce the structural and thermodynamic properties of bulk water and the polarization part of the potential was found to reproduce water's static dielectric constant.[16] The PSRWK model reproduces the evaporation energy of bulk water fairly well, although the pressure is too high. The radial distribution functions g_{OO}, g_{OH}, and g_{HH} for the PSRWK model compare well with experiment.[20] The dielectric constant of PSRWK was calculated by Sprik to be 86 ± 10, which is in reasonable agreement with the experimental value of 78.[21]

2.2. The WK Potential for Water. The Watanabe–Klein model,[15] denoted WK, was chosen as a good nonpolarizable model. In the WK model the Coulombic interactions are modeled by three partial charges two positive charges at the locations of the hydrogens, and a negative charge placed at an "M site" 0.15 Å from the oxygen. A Lennard-Jones interaction is centered on the oxygen. The charges and the distance between the "M site" and the oxygen were chosen to reproduce the estimated liquid phase dipole moment of water, and the LJ parameters were fit to the experimental density, energy, and pressure at room temperature. Unlike many water potentials, the WK potential fit to the energy includes an estimate of the polarization energy and the quantum mechanical librational energy.[22] A brief comparison of the parameters of PSRWK and WK is provided in Table 1. The WK potential adequately reproduces the thermodynamic and structural properties of bulk water. However, the estimated diffusion constant of the WK model is half the experimental value. The dipole moment of the WK model is 2.60 D, and its dielectric constant is estimated to be 80 ± 8. Table 2 shows that there are only a few small differences between the bulk thermodynamic and structural properties and dimer geometry and energy predicted by the WK and PSRWK model.

2.3. The Methane–Methane and Methane–Water Interactions. The methanes were approximated as spherically symmetric LJ molecules. The Me–Me LJ parameters were taken from Jorgensen.[23] Although the water–water LJ param-

(18) Allen, M. P.; Tildesley, D. J. Oxford University Press: Oxford, 1987.

(19) Martyna, G. The transformation given in eq 2.7 corrects the typo in eq 13 of ref 25. The authors must thank Dr. Glenn Martyna for providing the charge normal mode transformation.

(20) Soper, A. K.; Phillips, M. G. *Chem. Phys.* **1986**, *107*(1), 47–60.

(21) Bertolini, D.; Cassettari, M.; Salvetti, G. *J. Chem. Phys.* **1982**, *76*(6), 3285–3290.

(22) Kuharski, Robert A.; Rossky, Peter J. *J. Chem. Phys.* **1985**, *82*(11), 5164–5177.

Table 2. Comparison of the Properties of Water Predicted by the Sprik Model (PSRWK) and the Watanabe and Klein Model (WK)[b]

property	WK	PSRWK
U (kcal/mol)	-11.0^a	-11.1
P (kbar)	0.1	0.6
U_{dimer} (kcal/mol)	-5.1	-5.7
r_{dimer} (Å)	2.89	2.85
ϵ	80 ± 8	86 ± 10
D (10^{-9} m^2 s^{-1})	1.1 ± 0.3	2.4 ± 0.3

[a] Energy quoted without quantum correction of ref 22. [b] This table is adapted from ref 16.

eters for PSWRK and WK are different, the same Me−W LJ parameters were used in order to eliminate any differences in the solute−solvent interactions. These parameters were the same as those by Smith and Haymet.[10] Any differences observed between the PMF for PSRWK and WK will thus be due solely to the water model under consideration. The LJ parameters used are displayed in Table 3.

3. Simulation Methods

3.1. Molecular Dynamics Algorithm. The PSRWK model was simulated by an extended Lagrangian technique in which the fluctuating charges are treated as an auxiliary set of dynamical degrees of freedom with fictitious velocities and kinetic energies. The equations of motion for both kinds of degrees of freedom are integrated simultaneously using standard techniques. The rigid bond constraints are applied using RATTLE,[24] and the constraint of zero total charge is satisfied by using the alternate polarization coordinates described in section 2.1.

In order to compute the Helmholtz free energy, constant temperature molecular dynamics was performed. It has been shown by Sprik[25] that in order for PSRWK to produce the correct time scale for the dynamics, the charge motion must be adiabatically separated from the molecular motion of the waters. This is consistent with the notion that the fluctuating charges are, in some general way, modeling the true polarization fluctuations of the water's electron cloud which should rapidly readjust to changes in the positions of the molecules. In order to keep the charges cold, three separate Nosé thermostats are needed—one for the molecular rotations set at 300 K, one for the molecular translations also set at 300 K and one for the charges set at 5 K. The thermostats are coupled to the system as a frictional process using a second-order formulation of Hoover's equations.[26] The second-order equations were used in place of the mixed first- and second-order equations of Sprik because they can be integrated by a modification of the velocity Verlet with RATTLE algorithm. It must be noted that these equations of motion do not preserve the total energy of the extended system. There is, however, a good constant of the motion[26] which is given by

$$K_{\mathrm{PSRWK}} = \frac{1}{2}\sum_{i=1}^{N}\sum_{\alpha=\mathrm{O},H_1,H_2} m_{i\alpha}\dot{r}_{i\alpha}^2 + U(\{\mathbf{r}_{i\alpha}\}) + \frac{1}{2}Q_{\mathrm{trans}}\dot{\eta}_{\mathrm{trans}}^2 + \frac{1}{2}Q_{\mathrm{rot}}\dot{\eta}_{rot}^2 + \frac{1}{2}Q_{\mathrm{pol}}\dot{\eta}_{pol}^2 + 3Nk_BT_{\mathrm{trans}}\eta_{\mathrm{trans}} + 3Nk_BT_{\mathrm{rot}}\eta_{\mathrm{rot}} + 3Nk_BT_{\mathrm{pol}}\eta_{\mathrm{pol}} \quad (3.11)$$

where the η's are thermostat variables and the Q's are corresponding fictitious masses when all of the thermostats have the same temperature.

The masses, Q_κ, of the thermostats are best expressed in terms of relaxation times, $Q_\kappa = nK_BT\tau_\kappa^2$. Sprik[16] reported the rotational relaxation time, τ_{rot}, to be 35 fs, the translational relaxation time, τ_{trans}, to be 140 fs, and the charge fluctuation relaxation time, τ_{pol}, to be 8.5 fs. In order to achieve stable integration, however, we found here that the mass of the bath associated with the polarization as well as the mass of the polarization degrees of freedom, had to be reduced by a factor of 10 from the published values, yielding a relaxation time for the polarization of 2.7 fs.

The constant temperature velocity Verlet with RATTLE algorithm is due to Martyna[27] and is detailed in ref 28. It was used in all of the simulations. In every case, adequate temperature control was achieved.

3.2. Treatment of Long-Range Coulomb Forces. Both the polarizable and nonpolarizable water models involve Coulomb interactions. To properly account for the long-range nature of these forces, Ewald summation[18,29,30] was used in all of the simulations. Because the fluctuating charges in the PSRWK model are represented by Gaussian charge distributions, a slight modification of the standard formula is needed. In our simulations the real-space cutoff, α, was taken to be $6.0/L$ for all the simulations. The reciprocal space vectors $\{\mathbf{G}\}$ were distributed in a hemisphere, and their maximum length was taken to be $8\pi/L$. These parameters correspond to the use of approximately 150 reciprocal space vectors.

The PSRWK model is one of the most expensive models of water to simulate. Recently, a new polarizable model of water was introduced[31] which treats all charges as dynamical variables. This new model requires much less cpu time than the PSRWK model. It runs only 10% slower than fixed charge models. Had this model been available at the time we initiated this study it would have been used in place of the PSRWK model.

3.3. Computation of the Potential of Mean Force. Several methods can be used to determine the potential of mean force (PMF) between two methane molecules, $W(r)$.[3,10,32] The full PMF is computed from the windowed solute−solute distribution functions by a method due to Bader.[33] The set of overlapping solute−solute distribution functions, $\{g_\mu(r)\}$, computed using the set of restraining potentials, $\{\Phi_\mu(r;r_\mu)\}$, are determined from simulations. For the problem of two LJ particles dissolved in water, we used a quadratic potential in some windows

$$\Phi_\mu(r;r_\mu) = \frac{1}{2}k_\mu(r - r_\mu)^2 \quad (3.12)$$

and a quartic function in others windows

$$\Phi_\mu(r;r_\mu) = \frac{1}{4}k_\mu(r - r_\mu)^4 \quad (3.13)$$

The quartic restraining potential is flatter around r_μ than the quadratic potential (eq 3.12) while rising more sharply at the edges. These properties allow the force constant, k_μ, to be made large enough to adequately restrain the solutes to a narrow

(23) Jorgensen, W. L.; Madura, J. D.; Swenson, C. J. *J. Am. Chem. Soc.* **1984**, *106*(22), 6638−6646.
(24) Andersen, H. C. *J. Computational Phys.* **1983**, *52*, 24−34.
(25) Sprik, Michiel; Klein, Michael *J. Chem. Phys.* **1988**, *89*(12), 7556−7560.
(26) Martyna, Glenn J.; Klein, Michael L.; Tuckerman, Mark *J. Chem. Phys.* **1992**, *97*(4), 2635−2643.
(27) Martyna, G. Private communication.
(28) M. H. New Ph.D. Thesis, Columbia University, 1994.
(29) Hansen, J.-P. North-Holland, Amsterdam, 1986; pp 89−129.
(30) deLeeuw, S. W.; Perram, J. W.; Smith, E. R. *Proceedings of the Royal Society, London A* **1980**, *373*(1752), 25−56.
(31) Rick, S. W.; Stuart, S. J.; Berne, B. J. *J. Chem. Phys.* **1994**, *101*, 6141.
(32) Beveridge, D. L.; DiCapua, F. M. Annual Reviews, Inc., 1989.
(33) Joel Bader Ph.D. Thesis, University of California, Berkeley, 1992.

window without unduly affecting the structure near the center of the window. For relatively flat regions of the PMF, the quartic restraining potential was found to be better at confining the solutes to a narrow window of interparticle distances. Similarly, near the peak of a sharp barrier, the quartic potential was better able to keep the system localized on the barrier than the quadratic restraining potential. From eq 3.12, the set of potentials of mean force, $\{W_\mu(r)\}$, are determined

$$W_\mu(r) = -k_B T \log g_\mu(r) - \Phi_\mu(r;r_\mu) + K_\mu \quad (3.14)$$

where $\{K_\mu\}$ is a set of (unknown) proportionality constants. To avoid the estimation of the K_μ, and to include data from the overlaps between the distributions, we compute the derivative of the windowed PMF by differentiating eq 3.14

$$F_\mu(r) = dW_\mu(r)/dr \quad (3.15)$$

An approximation to the derivative of the full PMF, over the entire separation range, may then be computed as a weighted sum over the $F_\mu(r)$

$$F(r) = \frac{\sum_\mu \mathbf{w}_\mu(r) F_\mu(r)}{\sum_\mu \mathbf{w}_\mu(r)} \quad (3.16)$$

The $\mathbf{w}_\mu(r)$ are a set of weighting functions. We have taken

$$\mathbf{w}_\mu(r) = g_\mu(r) \quad (3.17)$$

although other choices are possible. This choice of weighting functions emphasizes information from well-sampled regions of the windows. Finally, the full PMF is reconstructed by integration

$$W(r) = \int_{r_{min}}^{r} F(r')dr' + W_0 \quad (3.18)$$

where W_0 is a constant which sets the zero of free energy.

A detailed exposition of an implementation of the algorithm used to compute the potentials of mean force, as well as the full error analysis, may be found in ref 28.

For the polarizable water model, all computations were started from a neat configuration of 216 molecules in a 18.626 Å box that had been equilibrated for 40 ps after starting from an ice-like tetrahedral lattice. The two waters closest to the center of the simulation box were then "mutated" into methanes, and the water−methane system was then equilibrated for 14 ps more. A combination of quartic and quadratic restraining potentials were used. Each window was simulated for 30 ps. The windows using the quadratic restraining potential were centered at 3.0 and 4.0 Å, while quartic restraining potential was used for the windows centered at 5.0, 5.5, 6.0, 6.5, 7.0, and 7.5 Å. This large number of windows ensured adequate overlap between the resulting intersolute distance distributions. The quadratic restraining potentials used a force constant of 2.4 kcal/mol/Å^2, and the quartic restraining potentials used a force constant of 38.6 kcal/mol/Å^4.

For the nonpolarizable model, fewer windows were used. For simplicity, only quartic restraining potentials were used because they produced distributions that were better overlapped, for the small number of windows used, than those that would have been produced using quadratic windows. They were centered at 4.0, 5.0, 6.0, and 7.0 Å. The force constant used for all the windows was 38.6 kcal/mol/Å^4.

The WK simulations were started from a configuration of 216 molecules that had been equilibrated for 80 ps from an ice-like lattice. Each window was simulated for 60 ps. Longer simulations were required for the WK potential since its diffusion constant is roughly half of the PSRWK diffusion constant.

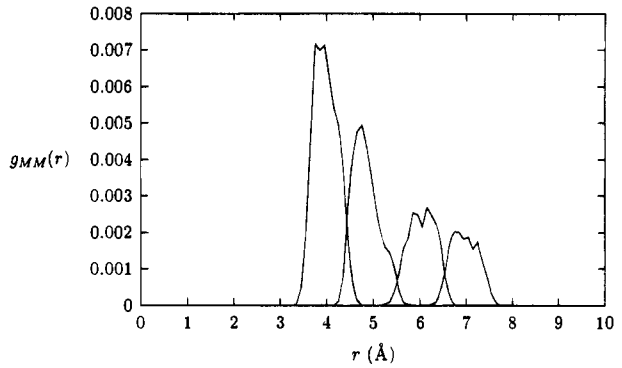

Figure 1. The raw solute−solute distance distribution functions as computed for the WK model.

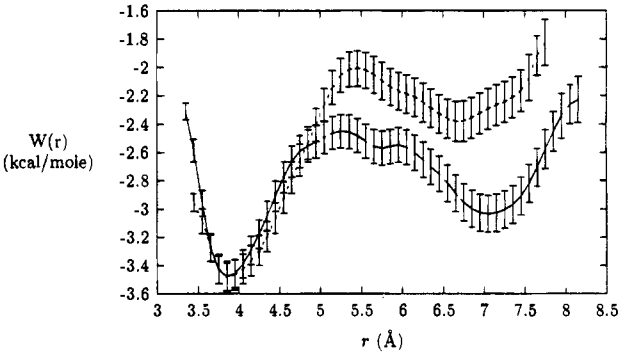

Figure 2. A comparison of the smoothed PMF for two methanes in water for PSRWK and WK with the computed (1σ) error bars included. The solid line is the PSRWK result. The dashed line is the WK result. The depths of the first minima have been set equal.

4. Results

The raw intersolute distance distributions for the nonpolarizable water model are shown in Figure 1. The potentials of mean force for the two water models are presented in Figure 2. These PMFs have been slightly smoothed by averaging points over their nearest and next nearest neighbors. All error bars are reported as $\pm 1\sigma$. For both of these figures, the energies of the contact pair minimum for the two water models have been set equal.

From Figure 2, it is clear that the solvent-separated minimum of the polarizable water model is quite deep and lies below the solvent-separated minimum of the nonpolarizable model (when both contact pair minima are set equal). The height of the barrier separating the contact pair from the solvent-separated pair, as measured from the bottom of the contact pair well, is 1.0 ± 0.2 kcal/mol for PSRWK and 1.5 ± 0.2 kcal/mol for WK. The depth of the second minimum, as measured from the barrier, is 0.6 ± 0.2 kcal/mol for PSRWK and 0.4 ± 0.2 kcal/mol for WK. The energy difference between the two minima is 0.5 ± 0.2 kcal/mol for PSRWK and 1.1 ± 0.2 kcal/mol for WK.

These data show that the nonpolarizable model does, indeed, have a higher barrier separating the solvent-separated state from the contact pair state. Additionally, the nonpolarizable model considered here has a larger difference in free energy between the solvent-separated and contact pair states than the polarizable model. Finally, the solvent-separated minimum in the polarizable model is slightly deeper than that of the nonpolarizable model.

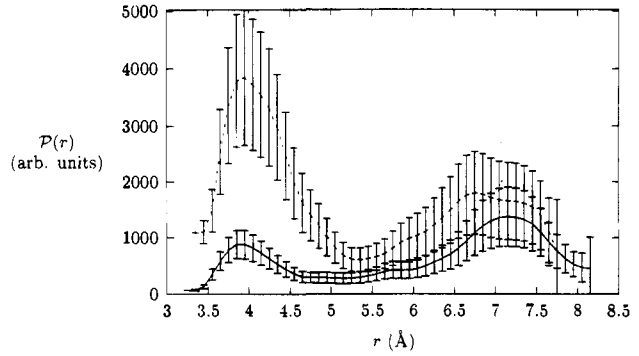

Figure 3. The unnormalized probability of finding the solutes a distance r apart in the fluid. The solid line is the PSRWK result. The dashed line is the WK result. The first minima of the potentials of mean force have been set equal.

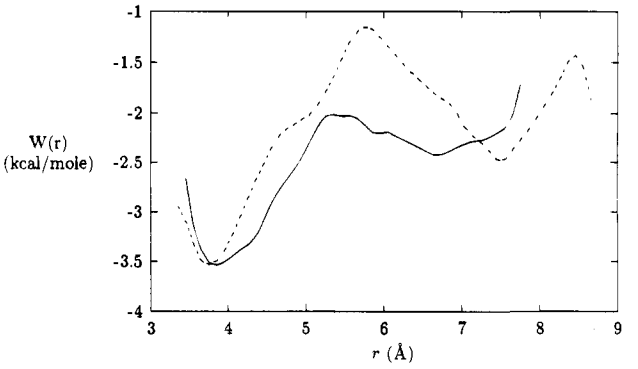

Figure 4. Comparison of potentials of mean force for the WK potential computed using Ewald summation (solid line) and spherical truncation (dashed line) boundary conditions.

The probability density that the two solutes will be a distance r apart in the fluid is given by

$$\mathscr{P}(r) \propto 4\pi r^2 e^{-W(r)/k_BT} \tag{4.19}$$

This probability density is displayed in Figure 3. For the polarizable model, the solvent-separated pair is more probable than the contact pair. Surprisingly, for the nonpolarizable model, the relative probabilities are reversed, and the contact pair is the more probable system configuration. This result is reflected in the values of the equilibrium constant for the pseudoreaction that takes a contact pair to a solvent-separated pair, eq 1.1, which may be computed from the intersolute distance probability, $\mathscr{P}(r)$[2]

$$K_{eq} = \int_{r_c}^{r_{max}} \mathscr{P}(r)dr \Big/ \int_{r_{min}}^{r_c} \mathscr{P}(r)dr \tag{4.20}$$

Choosing $r_c = 5.5$ Å, the probability distributions shown in Figure 3 yield

$$K_{eq}(\text{PSRWK}) = 2.3 \pm 0.3 \tag{4.21}$$

$$K_{eq}(\text{WK}) = 0.7 \pm 0.2 \tag{4.22}$$

Pangali *et al.*[2] have pointed out that this computation is very sensitive to the location of r_{max}, which, ideally, should be between the second and third maximum of $\mathscr{P}(r)$. For the computation of the intersolute distance probability, $r_{min} = 3.25$ Å, $r_c = 5.5$ Å, and $r_{max} = 8.15$ Å, ones using ST2 were for krypton-like particles. However, since the krypton−krypton potential used had a larger width parameter ($\sigma_{KrKr} = 4.12$ Å) and a deeper well ($\epsilon_{KrKr} = 171$ K) and the krypton−water potential had a smaller well depth ($\epsilon_{KrW} = 77.8$ K) than the potentials used in our study, one can still conclude that both the PSRWK and WK models promote contact pairing to a greater degree than ST2. Furthermore, the WK model seems to induce the aggregation of two apolar solutes which is in marked contrast to other nonpolarizable, pair-additive water potentials for which the solvent-separated state is more probable.[2,9] This raises the important question: Do potential models, like the WK and SPC/E models, based on parameters corrected for the polarization energy, always promote contact pairing over solvent-separated pairing?

Although we did not truncate the potential in the foregoing, it is of interest to determine what the effect of potential truncation could be on the PMF. Because the PSRWK simulations are very cpu intensive we only investigate this question using the WK potential. Results from our previous simulations of the WK potential using Ewald boundary conditions are compared with simulations in which the Coulombic interactions are spherically truncated at 8.5 Å in Figure 4. The potential of mean force for the truncated WK potential was computed using nine quartic windows centered at 4.0, 4.5, 5.0, 5.0, 6.0, 6.5, 7.0, and 8.0 Å using a force constant of 77.1 kcal/mol/Å^4. The simulations were started from a configuration of 216 molecules that had been equilibrated from an ice-like structure for 80 ps. Statistics were then collected for each window for 120 ps. These results indicate that the use of spherical truncation boundary conditions can substantially raise the barrier between the contact pair and the solvent-separated pair and change the position of the two minima. Spherical truncation significantly perturbs the PMF in the simulation based on the WK potential thus it is probable that spherical truncation will also give erroneous PMFs in the closely related polarizable model potential. Because polarizable models are more sensitive to boundary conditions, it is expected that the effects of spherical truncation boundary conditions on the potential of mean force for a polarizable model will be more serious.

In light of these findings one must question the validity of calculations of the PMF using spherical truncation of the water−water potential as was done in many published simulations. It may well be that the WK potential is uniquely sensitive to boundary conditions, but we doubt this. These observations raise serious questions about the use of spherical truncation for calculating PMFs—questions that should be addressed more frequently in simulations.

Other truncation schemes have been introduced. For example, the Coulomb potential has been replaced by a damped Coulomb potential.[34,35] Prevost *et al.*[35] have compared simulations on neat water using this scheme with simulations using Ewald boundary conditions. They found that the damped Coulomb simulations give results very similar to the full Ewald potential for neat water. This is the scheme used by Van Belle and Wodak[12] in their calculation of the PMF for two methane molecules in water. Unfortunately these results were not compared with Ewald simulations to verify that subtle effects do not give rise to differences.

5. Conclusions

The simulations reported here are used to compare the PMF for two spherical methane molecules in a nonpolar water model (WK) and in a corresponding polarizable water model (PSRWK) for the same Me−W interaction. These two water models have essentially the same dielectric and structural properties. The

(34) Brooks, C.; Pettitt, B. M.; Karplus, M. *J. Chem. Phys.* **1985**, *83*, 5897.

(35) Prevost, M.; van Belle, D.; Lippens, G.; Wodak, S. *Mol. Phys.* **1990**, *71*, 587.

simulations are performed using full Ewald boundary conditions in order to avoid artifacts due to various truncation schemes. The results of these simulations are summarized below.

The PMF in the polarizable (PSRWK) model is found to be qualitatively different from the nonpolarizable (WK) model. The polarizable model favors solvent-separated pairing, whereas the nonpolarizable model favors contact pairing. Because the Me−W interaction is taken to be identical in the polarizable and nonpolarizable models, the differences observed in the PMF for these two models can be ascribed to the differences in the water−water interactions. If the parameter ϵ_{Me-W} is made smaller in the polarizable model than in the nonpolarizable model, as was done in the study of van Belle and Wodak, the solvent-separated pairing would be reduced.

The PMF in the nonpolarizable (WK) model of water is found to be qualitatively different from the PMF found in other nonpolarizable water models (such as SPC, ST2, TIP4P). The Me−Me contact pair is found to be more probable than the Me−H_2O−Me solvent-separated pair. The equilibrium constant for the transformation specified by eq 1.1 is found to be $K_{eq}(WK) = 0.7 \pm 0.3$ compared to the value of $K_{eq} = 3.0$ found by Pangali *et al.* for a slightly different apolar sphere in ST2 water which favors solvent-separated pairing. The potential parameter, ϵ_{W-W}, for the O−O interaction in the WK model was parameterized based on the inclusion of correction factors to the internal energy due to the quantum mechanical nature of the librations and the energy needed to polarize the water molecules.[22] The bulk internal energy predicted by the WK model determined from the MD simulation is −11.0 kcal/mol. When the polarization energy (the energy to change the gas phase charges to liquid state charges) is added, one obtains the experimentally determined internal energy of bulk water is −9.9 kcal/mol.[36] The WK model is therefore roughly 10% more strongly bound than other nonpolarizable models[36,37] which ignore the polarization energy. Because the water molecules interact more strongly in the WK model, this model should be more solvophobic toward the pair of methane molecules than the other models, thus inducing more contact pairing. This is precisely what is observed. Since all of these other models give qualitatively different results for the PMF than the WK model, that is, all of them predict that the solvent separated pair Me−H_2O−Me is more probable than the contact pair Me−Me, we expect that other nonpolarizable models, such as the SPC/E model, which are also parametrized based on the polarization energy correction, will also give more stable contact pairing than solvent separated pairing.

The potential of mean force computed for the WK potential displays a higher barrier between the solvent-separated and contact pair minima and a shallower solvent-separated minimum than that computed using PSRWK. Precise quantitative comparisons are not possible at this time due to the large statistical uncertainties associated with the calculations.

When the nonpolarizable model water−water potential (WK) is spherically truncated at an O−O separation of 8.5 Å, the PMF is found to be very different from the results of full Ewald boundary condition simulations. Prevost *et al.* use a different "truncation scheme".[35] Here we find that solution properties like the PMF are quite sensitive to the truncation scheme used. Thus one cannot necessarily trust predictions made using potentials truncated at such distances. At this truncation distance water molecules in contact with one solute molecule will not interact with the water molecules in contact with the other solute molecule when the two solutes are in contact, but these water molecules can interact with a water molecule between the two methane molecules in the solvent-separated pair Me−H_2O−Me.

Table 3. LJ Parameters for the Water−Water, Methane−Methane, and Water−Methane Potentials

interaction	σ (Å)	ϵ (K)
water−water (PSRWK)	3.19	101.0
water−water (WK)	3.18	141.5
methane−methane	3.73	147.5
water−methane (all)	3.44	107.3

The reasons for the differences in the PMF for the polarizable (PSRWK) potential and the nonpolarizable (WK) potential are not yet clear. Nevertheless, we list several observations and conjectures that might help to clarify these findings.

(a) In nonpolarizable water, electrostatic interactions cause the waters to hydrogen bond. If a hydrogen-bonded water molecule is forced to rotate around an axis perpendicular to the molecular plane its dipole moment must rotate with it. This rotation will then raise the electrostatic energy of the system. Such distortions of the hydrogen bond network are therefore resisted.

In polarizable water, electrostatic interactions still cause the waters to hydrogen bond. If a hydrogen-bonded water molecule is forced to rotate around an axis perpendicular to the molecular plane only its permanent dipole moment must rotate with it. The induced moments are free to point in other directions, consequently, rotation of the permanent dipole will raise the electrostatic energy, but the induced dipole−dipole interaction need not increase. In polarizable water, rotation of a water molecule should not raise the electrostatic energy as much as in nonpolarizable water and such distortions of the hydrogen-bond network are not likely to be resisted as much as in the nonpolarizable water models.

Notwithstanding these two facts, the structure, energetics, static dielectric properties, and hydrogen bonding in neat liquid are observed to be similar for polarizable and nonpolarizable water molecules. How can this be true given that it costs less electrostatic energy to distort the hydrogen-bond network in the polarizable model than in the nonpolarizable model? This might be due to the different LJ parameters used for the O−O interactions in these two models (see Table 3).

(b) In the solvent-separated pair, Me−H_2O−Me, the water molecule shared between the two Me molecules will hydrogen bond to water molecules forming the two clathrate cages containing each of the Me molecules. Although not shown here, it has been found that the distribution function for the total dipole moment of the bridging water molecule in polarizable water is broader than for the other water molecules in the shell.[28] This bridging water molecule will be able to explore more configurational states, and this will lead to a larger entropy in the solvent-separated state for the nonpolarizable model than for the polarizable model. Should this be the case, the polarizable model should give rise to a more stable solvent-separated state than the nonpolarizable model.

(c) In the contact pair state, all of the waters in the solvation shell of the pair of Me molecules will be essentially equivalent, and the hydrogen bond profiles will be essentially the same for the polarizable and nonpolarizable models. Thus there will be no difference in the free energies of contact pairing in the polarizable and nonpolarizable fluids. This is verified by the fact that the total dipole moment on these shell molecules are the same for the polarizable and nonpolarizable models.[28]

The qualitative results observed in our polarizable model are in complete disagreement with those recently published by van

(36) Jorgensen, W. L.; Chandrasekhar, J.; Madura, J. D.; Impey, R. W.; Klein, M. L. *J. Chem. Phys.* July **1983**, *79*(2), 926−935.

(37) Reimers, J. R.; Watts, R. O.; Klein, M. L. *Chem. Phys.* **1982**, *64*(1), 95−114.

Belle and Wodak[12] for the PSPC model. In the PSPC model the solvent-separated minimum in the PMF of two methane molecules virtually dissappears. In trying to explain these differences it is important to note that (a) van Belle and Wodak use different Me−W potentials for the SPC and PSPC simulations of water, whereas we use the same Me−W potentials for the WK and PSRWK simulations. (b) Van Belle and Wodak truncate the water−water potential, whereas we use Ewald boundary conditions. Although it is completely possible that these methodological differences can play an important role in generating differences between our simulations and theirs, it is also possible that the observed qualitative differences are due to the very different potential models of water used. Nevertheless, it is worth discussing further how the methodological differences might effect the results.

Even if possible errors introduced by the truncation scheme used by Van Belle and Wodak are ignored, the difference in the Me−W interaction potential used by Van Belle and Wodak in the SPC and PSPC models may be sufficient to explain their observed disappearance of the solvent-separated minimum in the PMF of the polarizable fluid. The well depth of the Me−W potential used with the polarizable model (PSPC) was 0.019 kcal/mol (8.9%) smaller than that used with the nonpolarizable model. As discussed by Pratt and Chandler[38] and later by Smith and Haymet[10] a weakening of the solute−water interaction will destabilize the solvent-separated pair relative to the contact pair.

Pratt and Chandler have introduced a set of integral equations for the calculation of the PMF of two spheres in water. To calculate the PMF from these equations one must input the O−O radial distribution function of water, $g_{O-O}(r)$, and the direct correlation function, $C_{Me-O}(r)$, for the solute-water interaction. Pratt and Chandler modeled the methanes as hard spheres and thus use a Percus−Yevick closure for the $C_{Me-O}(r)$. They then substitute the experimentally determined $g_{O-O}(r)$ and solve the integral equation for the PMF. This semiempirical theory has been very useful in understanding the qualitative properties of the hydrophobic interaction. For continuous potentials one can introduce the mean spherical approximation, $C_{Me-O}(r) = -\beta U_{Me-W}(r)$, into these equations. We have computed the $g_{O-O}(r)$'s for simulations of neat WK water and neat PSRWK water. These functions are essentially indistinguishable except for very small differences. The $U_{Me-W}(r)$ are the same for both of the simulations reported in this paper. Thus if we invoke the MSA approximation and the Pratt−Chandler integral equations, we would predict that the PMFs for the WK and PSRWK should be essentially identical. The simulations show that the PMFs for these two models are very different. Why? Four possibilities suggest themselves: (a) The simulations are in error. (b) The integral equations are accurate, but the MSA closure is in error. (c) The MSA closure is correct, but the integral equation is incorrect for polarizable fluids. (d) Subtle differences in $g_{O-O}(r)$ at long range might give rise to important differences in $S_{O-O}(k)$ and thus to different PMFs. Since the inversion of the OZ equations depends on the structure factor rather than on $g_{O-O}(r)$, this may give rise to differences in the PMFs.

It is our belief that the simulations are not in error. It is quite possible that even if $U_{Me-W}(r)$ is the same for the two simulations, the MSA closure may be incorrect, and the $C_{Me-W}(r)$'s may be different in the two simulations. In this case the OZ equations introduced by Pratt and Chandler can be regarded as defining the direct correlation functions. Then the MSA closure may be worse than other possible closures, and the direct correlation functions may depend on the other correlation functions, $g_{OH}(r)$ and $g_{HH}(r)$. It is difficult to determine the structure function at small k for simulated systems so that we cannot say if item (d) is responsible for the differences. Lastly, if one formulates the problem in terms of Gaussian density and polarization fields[39] and includes the coupling between the divergence of the polarization field and the density field, it is possible that after integrating out the polarization field one will obtain a different integral equation for the PMF for the polarizable solvent than for the nonpolarizable solvent.

One factor that has not been treated here is the effect of including the polarizability of the solutes. The polarizability of methane is 2.60 Å^3,[40] which is larger than that of water (1.44 Å^3). At contact, when the methanes are close enough together to experience very similar electric fields, their repulsion should be enhanced. As the solutes are separated, the correlation between their local electric fields should be reduced. The additional solute−solute repulsion originating from induced dipole-induced dipole interactions should then be reduced. Overall, the effect would be to stabilize the solvent−separated pair. This effect has already been observed in simulations of polarizable Xe atoms in nonpolarizable water.[41]

Acknowledgment. This work was supported by a grant from the National Institutes of Health (GM43340) and from the NIH Division of Research Resources (SP41RR06892). We wish to thank Professor David Chandler for illuminating discussions about possible approaches to generalizing the Pratt−Chandler theory to polarizable fluids and for useful comments on an earlier version of the manuscript.

JA944140I

(38) Pratt, L. A.; Chandler, D. *J. Chem. Phys.* **1980**, *73*(7), 3434−3441.
(39) Chandler, D. *Phys. Rev. E* **1993**, 2898.
(40) Hirschfelder, J. O.; Curtiss, C. F.; Byrd, R. B. John Wiley and Sons, Inc.: New York, 1954.
(41) Backx, P.; Goldman, S. *Chem. Phys. Lett.* **1985**, *113*, 578.